^{96}Zr(^{13}C,4nγ):XUNDL-3 2019Ti02

Compiled (unevaluated) dataset from 2019Ti02: Phys Rev Lett 122, 062501 (2019).
Compiled by B. Singh (McMaster); March 2, 2019.
This paper reports evidence of transverse wobbling mode of excitation based on one-neutron configuration.
2019Ti02: the ^{13}C beam was provided by the Vivitron accelerator of the IReS, Strasbourg. Target=86% enriched ≈0.6 mg/cm^2 thick ^{96}Zr foil. Measured Eγ, Iγ, $\gamma\gamma$-coin, $\gamma\gamma(\theta)$(DCO), $\gamma\gamma$(linear polarization) using EUROBALL IV array of 15 Cluster Ge detectors at backward angles and 24 Clover Ge detectors at 90° to the beam direction, and the DIAMANT array of 88 CsI detectors for charged particles. Deduced rotational bands, multipolarities, mixing ratios, configurations, and transverse wobbling mode of excitation. Comparison with constrained triaxial covariant density functional theory (CDFT) and quantum particle rotor model (PRM) calculations.
Authors mention that details of this work with full level scheme will be provided in a forthcoming publication (see reference 30 in the paper).

^{105}Pd Levels

E(level)[†]	J$^\pi$[‡]	$T_{1/2}$	Comments
0[#]	5/2$^+$[#]		
306[#]	7/2$^+$[#]		
442[#]	7/2$^+$[#]		
489[@]	11/2$^-$	36.1[#] μs *4*	
970[@]	15/2$^-$		
1357[&]	13/2$^-$		
1742[@]	19/2$^-$		
1961[&]	17/2$^-$		B(M1: 991γ)↓/ B(E2: 604γ)↓=0.162 μ_N^2/e^{2}b^2 *97*; B(E2: 991γ)↓ / B(E2: 604γ)↓=0.66 *18*. The M1 and E2 components of the 991γ are deduced from δ(E2/M1) for 991γ, and its γ-ray intensity.
2700[@]	23/2$^-$		
2775[&]	21/2$^-$		B(M1: 1034γ)↓/ B(E2: 814γ)↓=0.089 μ_N^2/e^{2}b^2 *26*; B(E2: 1034γ)↓ / B(E2: 814γ)↓=0.60 *9*. The M1 and E2 components of the 1034γ are deduced from δ(E2/M1) for 1034γ, and its γ-ray intensity.
2900[a]	21/2$^-$		
3073[#]	(21/2)$^+$[#]		
3694[&]	25/2$^-$		B(M1: 994γ)↓/ B(E2: 918γ)↓=0.029 μ_N^2/e^{2}b^2 *16*; B(E2: 994γ)↓ / B(E2: 918γ)↓=0.34 *7*. The M1 and E2 components of the 994γ are deduced from δ(E2/M1) for 994γ, and its γ-ray intensity.
3800[@]	27/2$^-$		
3859[a]	25/2$^-$		
4783[&]	29/2$^-$		
4952[@]	31/2$^-$		
4955[a]	29/2$^-$		
5847[&]	33/2$^-$		
6071[@]	35/2$^-$		
6995[&]	37/2$^-$		
7190[@]	39/2$^-$		
8297[&]	41/2$^-$		
8405[@]	43/2$^-$		

[†] From Eγ values.
[‡] From 2019Ti02, based on previous assignments for the yrast band, and multipolarities from DCO and POL data for the two new bands reported in the present work. Exceptions are noted.
[#] From ^{105}Pd Adopted Levels in the ENSDF database (Sept 2004 update). Level energies are rounded values.
[@] Band(A): Yrast $\nu h_{11/2}$,α=−1/2. Configuration=$\nu h^3_{11/2}$ after spin 27/2. This band interpreted as due to tranverse wobbling mode

Continued on next page (footnotes at end of table)

^{96}Zr(^{13}C,4nγ):XUNDL-3 2019Ti02 (continued)

^{105}Pd Levels (continued)

of excitation, with oscillation quantum number n=0, based on dominant interband E2 transitions of 991, 1034 and 994 keV.

[&] Band(B): $\nu h_{11/2},\alpha=+1/2$. Configuration=$\nu h_{11/2}\otimes\pi g_{9/2}^{-2}$ after spin 29/2. This band interpreted as due to tranverse wobbling mode of excitation, with oscillation quantum number n=1, based on dominant interband E2 transitions of 991, 1034 and 994 keV.

[a] Band(a): $\nu h_{11/2},\alpha=+1/2$. Signature partner of band based on $11/2^-$.

$\gamma(^{105}Pd)$

E_γ	E_i(level)	J_i^π	E_f	J_f^π	Mult.[‡]	δ[‡]	Comments
183[†]	489	$11/2^-$	306	$7/2^+$	M2[†]		
306[†]	306	$7/2^+$	0	$5/2^+$			
387	1357	$13/2^-$	970	$15/2^-$			
442	442	$7/2^+$	0	$5/2^+$	M1+E2	−0.37 *8*	
481	970	$15/2^-$	489	$11/2^-$			
604	1961	$17/2^-$	1357	$13/2^-$			
772	1742	$19/2^-$	970	$15/2^-$			
794	3694	$25/2^-$	2900	$21/2^-$	(E2)		
814	2775	$21/2^-$	1961	$17/2^-$	E2		
868	1357	$13/2^-$	489	$11/2^-$			
918	3694	$25/2^-$	2775	$21/2^-$	E2		
924	4783	$29/2^-$	3859	$25/2^-$			
939	2900	$21/2^-$	1961	$17/2^-$	(E2)		
958	2700	$23/2^-$	1742	$19/2^-$			
959	3859	$25/2^-$	2900	$21/2^-$			
983	4783	$29/2^-$	3800	$27/2^-$			
991	1961	$17/2^-$	970	$15/2^-$	E2+M1[#]	+1.8 *5*	
994	3694	$25/2^-$	2700	$23/2^-$	E2+M1[#]	+2.7 *6*	
1034	2775	$21/2^-$	1742	$19/2^-$	E2+M1[#]	+2.3 *3*	
1064	5847	$33/2^-$	4783	$29/2^-$	E2		
1084	3859	$25/2^-$	2775	$21/2^-$			
1089	4783	$29/2^-$	3694	$25/2^-$	E2		
1097	4955	$29/2^-$	3859	$25/2^-$			
1100	3800	$27/2^-$	2700	$23/2^-$			
1119	6071	$35/2^-$	4952	$31/2^-$			
1119	7190	$39/2^-$	6071	$35/2^-$			
1148	6995	$37/2^-$	5847	$33/2^-$			
1152	4952	$31/2^-$	3800	$27/2^-$			
1158	2900	$21/2^-$	1742	$19/2^-$	M1+E2		POL=−0.6 *3* for 1158+1159 doublet. δ: 0 to +0.5 or +1 to +2.4.
1159	3859	$25/2^-$	2700	$23/2^-$	M1+E2		POL=−0.6 *3* for 1158+1159 doublet. δ: 0 to +0.5 or +1 to +2.4.
1215	8405	$43/2^-$	7190	$39/2^-$			
1261	4955	$29/2^-$	3694	$25/2^-$			
1302	8297	$41/2^-$	6995	$37/2^-$			
1331	3073	$(21/2)^+$	1742	$19/2^-$	E1		

[†] From ^{105}Pd Adopted dataset in the ENSDF database (Sept 2004 update). Energies are rounded values.

[‡] From $\gamma\gamma(\theta)$(DCO) and $\gamma\gamma$(lin pol) data in 2019Ti02, unless otherwise stated. Sign of mixing ratio is positive when not explicitly stated in 2019Ti02, according to correspondence with J. Timar, March 2, 2019.

[#] Dominant E2 component in the 991, 1034 and 994 transitions between the n=0 and n=1 bands indicates wobbling mode of excitation.

^{96}Zr(^{13}C,4nγ):XUNDL-3 2019Ti02

Level Scheme

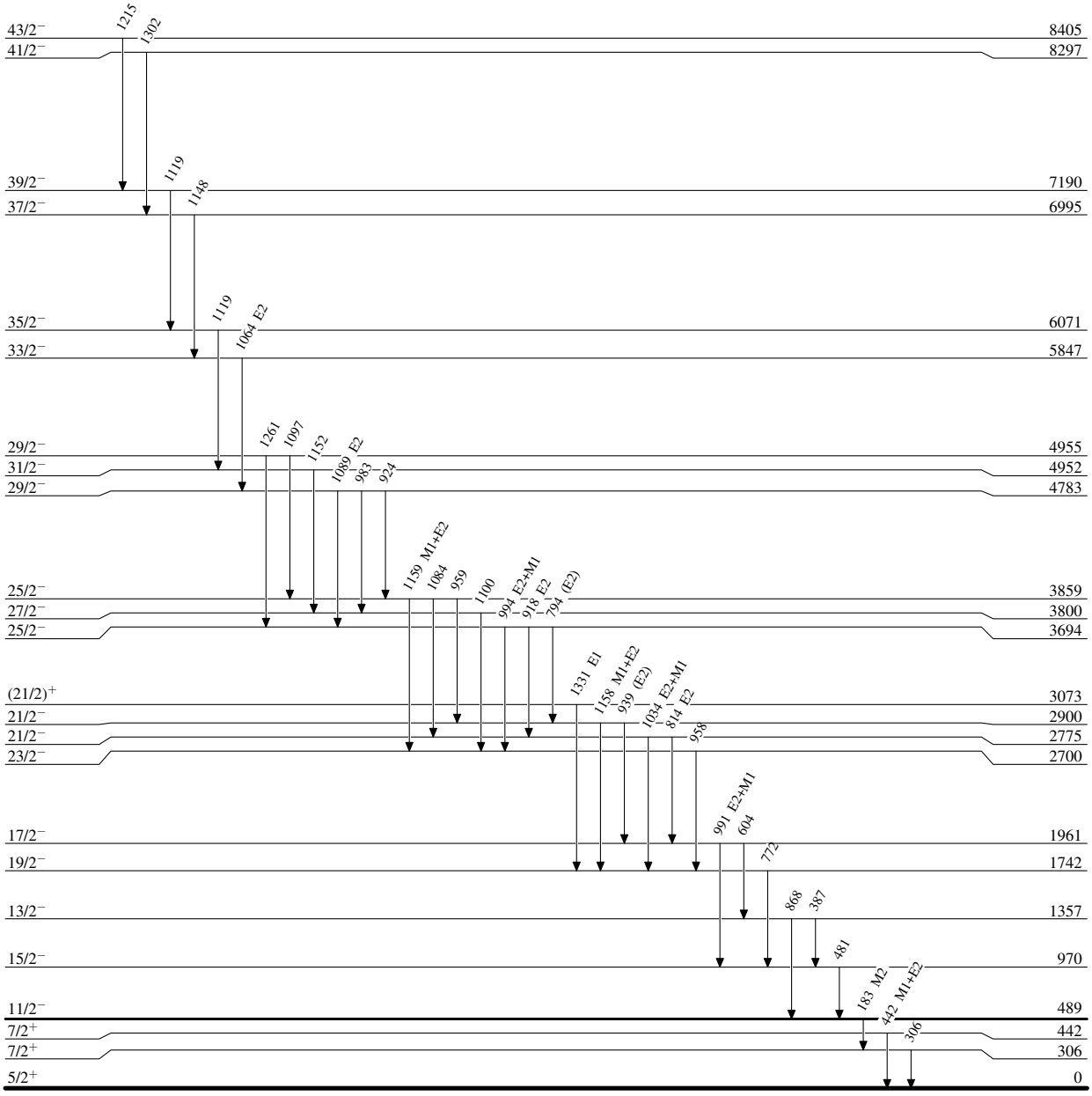

$^{105}_{46}Pd_{59}$

^{96}Zr(^{13}C,4nγ):XUNDL-3 2019Ti02

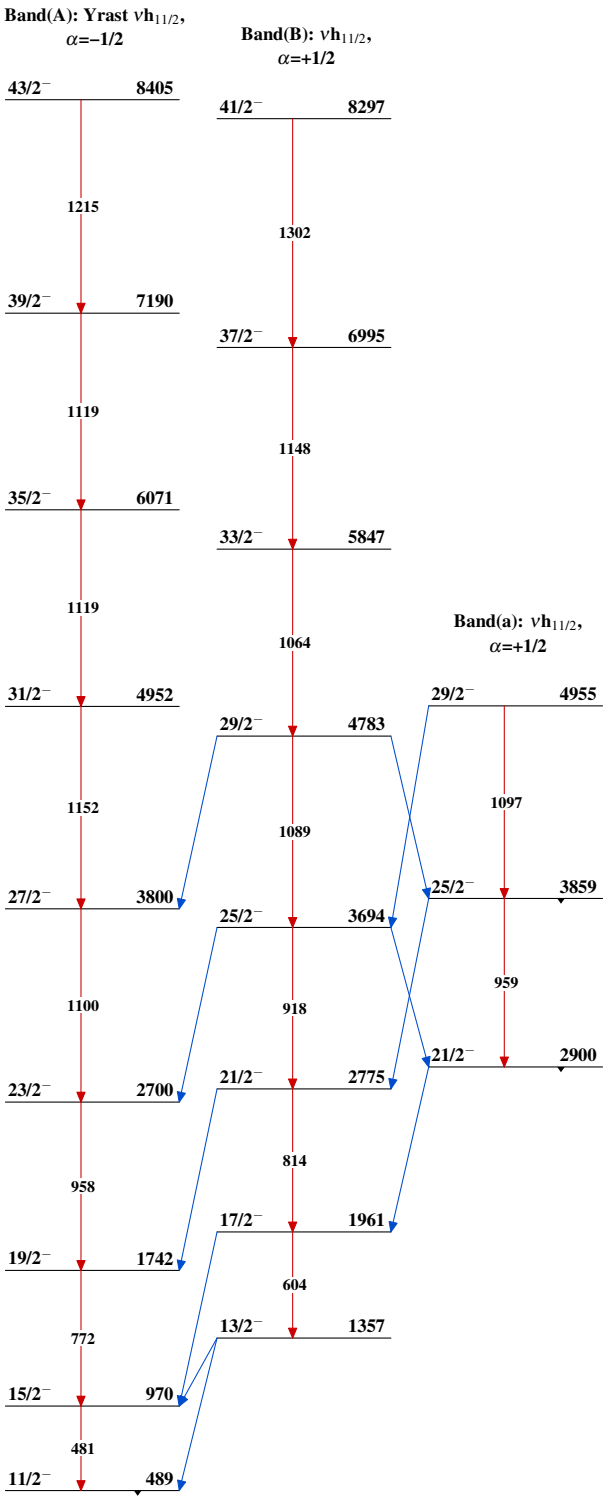

$^{105}_{46}Pd_{59}$